New inorganic–organic lamellar derivatives synthesized from H-RUB-18 and thermodynamics of cation sorption

Thaís R. Macedo and Claudio Airoldi*

A synthesized crystalline lamellar sodium RUB-18 was reacted with hydrochloric acid solution to exchange the original hydrated sodium cation on the interlayer space to obtain the acidic form, H-RUB-18, whose silanol groups on the surface favour covalent bond formation with the silylating agents 3-aminopropyltriethoxysilane (N) and N-3-trimethoxysilylpropyldiethylenetriamine (3N). Both new organofunctionalized nanostructured materials were characterized by means of elemental analysis, IR spectroscopy, X-ray diffraction patterns, NMR, thermogravimetry and scanning electron microscopy. The determined maximum amount of coupling reagents incorporated were 2.28 and 1.03 mmol g^{-1}, for RUB-N and RUB-3N, respectively. The H-RUB-18 basal distance of 0.75 nm expands to 0.94 and 1.10 nm in two successive steps of reaction. Covalent bond formation between the organosilyl groups and the inorganic layered backbone was confirmed by ^{13}C and ^{29}Si NMR, as evidenced by carbon chemical shifts of the pendant organic chains and by the Q^3 and Q^4 sites, in addition to T^2 and T^3 species, that correspond to carbon–silicon bond formation from the pendant coupling reagents covalently attached to the H-RUB-18 structure. These two new synthesized materials have the ability to extract divalent cations from aqueous solution, using a batchwise process. The same interaction was also followed through calorimetric titration and the thermodynamic data, with high entropic contributions, indicated favourable cation/basic centre interactions at the solid/liquid interface.

Introduction

Na-RUB-18 is one of the members of the hydrous sodium layered silicate groups, also containing makatite, kanemite, magadiite and kenyaite.[1] From the synthetic point of view, these compounds are usually prepared in laboratory in the sodium (sodic) form, with hydrated sodium cations located in the interlayer position, to maintain charge neutrality. Therefore, this precursor interlayered cation can easily be exchanged by protons, in dilute acidic solutions, to obtain layered silicic acids, which are very useful hosts for organo-modified material preparations, due to the presence of available reactive silanol groups, inside the self-organized sequence of layers.[2,3] This well-established layered arrangement with available silanol groups suggests a great variety of novel synthesized materials after chemical modification, using different synthetic procedures, aiming to design molecules grafted to the inorganic polymeric structure with new and desirable functionalities.[4]

Recently, for Na-RUB-18 the chemical composition was precisely determined as $Na_8Si_{32}O_{64}(OH)_8 \cdot 32H_2O$, with an interlayer distance and a layer thickness of 1.11 and 0.73 nm,[5] indexed as (001) and (100) diffraction planes, respectively, with the crystal structure details elucidated through X-ray

diffraction patterns and solid-state NMR spectroscopy.[1] In addition, makatite[6] and kanemite[7] layered compounds also had their structures elucidated, and the collected data enabled proposing structural models for magadiite and kenyaite, where the chemical condensation of the makatite-like layers is an idealized precursor structure, considering the SiO_4 tetrahedral units with different connectivities.[8] On the other hand the crystal structures of the layered silicic acids of magadiite and kenyaite remain unknown.

The structural building unit of the Na-RUB-18 silicate layer consists of four- and five-membered rings. This is the first time that this [5^4] cage, common for several high silica zeolites, has been observed in a layered silicate. The remaining four silicon atoms are bonded to hydroxyl groups or have a negative charge that is compensated by octahedrally coordinated sodium cations that form one-dimensional chains of octahedral edge-sharing [NaO_6] units. Weak and strong hydrogen bonds among the intercalated waters and the siloxane or with silanol groups are observed.[9]

The available silanol groups attached to the layered surfaces on the proposed silicic acid structures are comparable to those of a silica gel surface, where their reactivity enables the grafting of organic molecules onto the inorganic polymeric structure,[2,3] as previously observed for synthetic phyllosilicate,[10] crysotile fibers,[11] natural talc[12] and mesoporous silica.[13]

Organofunctionalized materials have been attracting interest due to the possibility of combining organic and inorganic components at the nanoscale level, offering favourable conditions to enhance new properties.[14] On the layered

Institute of Chemistry, University of Campinas, UNICAMP, P.O. Box 6154, Campinas, SP, 13084-971, Brasil.
E-mail: airoldi@iqm.unicamp.br; Fax: +55 19 3521 30 23;
Tel: +55 19 3251 3055

surface, organofunctionalization processes enable designing the construction of inorganic–organic nanostructured materials through the grafting procedure of silylating agents between the silicate layers, to obtain nanomaterials with the desired functionalities.[4,14] For example, an amine as free functional group in the end position on pendant chains covalently bonded to the surface can be a reactive site for chemical attachment of polymers.[15] In addition, amine-layered materials may also be applied for adsorption of heavy metals, dyes and also as supports for drug delivery.[16]

Taking into account the organofunctionalization of layered silicates, another feature is related to kanemite surface modification. As this as-synthesized structure consists of single layers of SiO_4 tetrahedra connected to six-membered rings, the layered arrangement gives structural flexibility. Thus, chemical modification of the kanemite surface causes structural changes in the layers, and new five- and six-membered rings can be formed. This high flexibility may be a disadvantage, resulting in materials with incomplete organofunctionalization and also not well-organized structures.[17] An advantage is the use of silicates composed of thick layers, such as Na-RUB-18, magadiite or kenyaite. Na-RUB-18 has thicker layers than kanemite, resulting in rigidity of the silicate plates,[5] to give materials with more crystalline and organized structures, which are dependent on the possible synthetic procedures. Acidic magadiite[18] was silylated with a series of chlorosilane coupling reagents. Also the silicic acid kenyaite[19] incorporated polymeric amines as curing agents for obtaining epoxy-layered silicate nanocomposites.

Earlier studies explored the immobilization of some short organoalkoxysilane pendant chains using alkylammonium derivatives of RUB-18 as intermediates, which enable the accommodation of larger molecules by prior interlayer expansion.[20,21] The present investigation reports direct H-RUB-18 interlayer organo-modifications with organo-alkoxysilanes, containing basic nitrogen atoms in the pendant chains, whose properties were evaluated for cation removal from aqueous solutions. This interactive process was followed through calorimetric titration and the thermodynamic data are closely related to cation/basic centre interactions at the solid/liquid interface for these new materials. The properties of the organo-modified derivatives obtained were also evaluated through different characterization techniques, such as elemental analysis, X-ray diffraction patterns, silicon and carbon NMR in the solid state, thermogravimetry, IR spectroscopy and scanning electron microscopy.

Results and discussion

Acidic RUB-18 presents available silanol groups distributed on the inorganic layers, being capable of incorporating silylating agents in the immobilization process, as extensively investigated for silica gel surfaces.[22] The synthesized silicic acid favours the bonding of the coupling reagents between the layers to perform the anchoring process, after prior drying in vacuo, to guarantee removal of physisorbed water molecules from the original material's surface. The elemental analysis values for carbon, hydrogen and nitrogen for the chemically modified derivatives are listed in Table 1. The successfully

silylated surfaces gave attached covalent pendant chains incorporated in the inorganic framework, the amount of which was calculated based on carbon atom content. The favourable result from the second cycle of the organofunctionalization reaction is illustrated when comparing the values obtained of 2.28 and 1.03 mmol g^{-1} (n_2) in relation to those from the first reaction that grafts 1.16 and 0.48 mmol g^{-1} (n_1) for N and 3N derivatives, respectively. These values for the grafting process represent an unequivocal proof of the anchoring of silane reagents at the surface of the acidic RUB-18 layered material.

The synthesized layered material Na-RUB-18 presents typical X-ray diffraction patterns, in agreement with the structure already reported,[9] as shown in Fig. 1(a). The lamellar structure is confirmed by peaks at 2θ 8.05° (1.10 nm), and 16.02° (0.55 nm), which are indexed to (001) and (002) diffraction planes, respectively. The layered crystalline material is directly observed by signals for 2θ between 23 to 30° range, corresponding to 3.86 to 2.97 nm. The success of the replacement of hydrated sodium ions by protons, during Na-RUB-18 acidification is confirmed by the basal spacing decreasing from 1.10 to 0.75 nm, as indicated by the 2θ value at 11.86°, as shown in Fig. 1(b). This decrease in basal spacing is in agreement with the loss of the bulkier solvated sodium ions in comparison to the proton in the exchange process.[1]

The X-ray diffraction patterns of the organofunctionalized materials with distinct pendant chains from the silane reagents showed the presence of the same reflections in the first silylation reaction, with the same basal spacing at lower 2θ values in relation to the starting material, H-RUB-18, as shown in Fig. 1(c) and (d). The basal distance obtained for both functionalized materials were 0.94 nm ($2\theta = 9.54°$), with an expansion of 0.19 nm, when compared to the starting acidic form. The second reaction, in the case of RUB-N, leads to no further change except for a decrease in intensity (Fig. 1(e)), while for RUB-3N a shift of 2θ to lower values of 8.05° was observed (Fig. 1(e) and (f)), which corresponds to an interlayer distance of 1.10 nm. Considering these interlayer space values it is possible to propose that those pendant organic chains are mostly bonded on the external surface of the material, since the expansions depend not only on the amount of silylating agent grafted, but also on the molecular size of the pendant group.[10] In the present case, the 3N pendant molecule is much larger when compared to the corresponding N pendant molecule, demonstrating also that there is a limit for interlayer increasing.

From the thermogravimetric curves for the sodic and acidic RUB-18 forms the percentages of mass loss obtained were 17.5 and 5.3%, which correspond to 9.72 and 1.57 mmol of water per gram of material, in agreement with previously reported data.[5] This difference is expected since the sodium interlayered sites were coordinated by water molecules. Through the obtained value for acidic RUB-18, it is possible to calculate 3.80 mmol g^{-1} of silanol groups on the surface, considering the unit cell of the acidic $H_2Si_8O_{17}\cdot1.57H_2O$ layered compound. The chemically modified structures showed mass losses of 13.7 and 15.6% for RUB-N and RuB-3N materials, respectively, after the second organofunctionalization reaction. These values can be attributed to the decomposition of fragments of the silylating agent, covalently bonded to the

Table 1 Basal distances for the first (d_1) and the second (d_2) reactions of organofunctionalization. Percentages of carbon (C), hydrogen (H) and nitrogen (N) obtained from elemental analysis for the final product. The amounts of silyl groups grafted to H-RUB-18 in the first (n_1) and the second (n_2) reactions calculated from elemental analysis. Those obtained from thermogravimetry (n_{Tg}) are for the final stage of synthesis

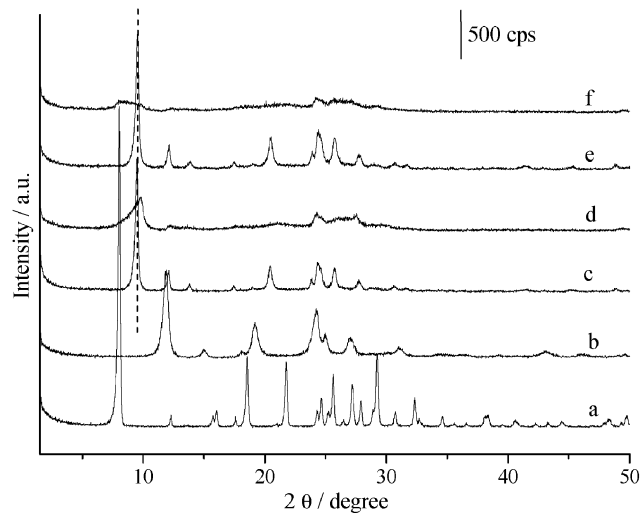| Material	d_1/nm	d_2/nm	%C	%H	%N	n_1/mmol g^{-1}	n_2/mmol g^{-1}	n_{Tg}/mmol g^{-1}
RUB-N	0.94	0.94	8.61	2.10	3.19	1.16	2.28	2.37
RUB-3N	0.94	1.10	10.16	3.02	4.34	0.48	1.03	1.09

Fig. 1 X-Ray diffraction patterns of Na-RUB-18 (a) and H-RUB-18 (b), products of first reaction for RUB-N (c), RUB-3N (d) and after the second reaction for RUB-N (e) and RUB-3N (f).

Fig. 2 Thermogravimetric curves of the organo-modified derivatives RUB-N and RUB-3N (b).

inorganic host. The larger pendant organic chain 3N resulted in a higher amount of decomposed chain while a higher temperature is required for decomposition. These percentages correspond to 2.37 and 1.09 mmol of silane decomposed, and are listed in Table 1 as n_{Tg}. These values correspond to 62.4 and 28.7% of silanol groups interacting covalently with the organo-compounds. The thermogravimetric curves obtained for the organo-modified derivatives are shown in Fig. 2. The first step of mass loss, up to 390 K, corresponds to the loss of water and alcohol, which is formed from the hydrolysis, during the organofunctionalization reaction (and also used in the washing process), giving amounts of 0.98 and 1.60 mmol g^{-1} for RUB-N and RUB-3N hybrids, respectively. The second stage, from 390 to 860 K, corresponds to the release of the silane reagent bonded to the surface, while the last step, starting at 860 K, is related to the loss of water molecules from condensation of the remaining silanol groups in the inorganic structure. The values of number of moles of attached molecules obtained from thermogravimetric data calculation, n_{Tg}, were close to those from elemental analysis, as listed in Table 1. This agreement from different calculation procedures is a clear indication of a well-behaved system.

Scanning electron microscopy of the acidic and organically modified RUB-18 forms are shown in Fig. 3. The images reveal the plate-like morphology of both samples, which is supposed to be related to the layered materials, as established before.[22] Furthermore, after chemical modification the morphology was still preserved, with little exfoliation, due to the silylation process in the RUB-3N material, which is also supported by X-ray diffraction data, as shown in Fig. 3(b).
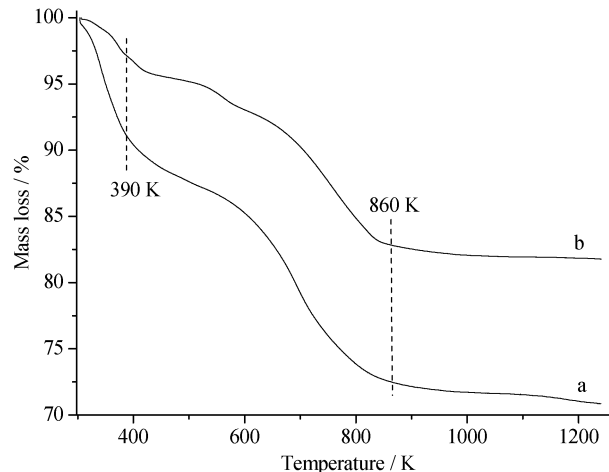
The IR spectrum of the layered sodium RUB-18 is shown in Fig. 4(a). The main bands are related to the inorganic backbone structure, present in the 1400 to 500 cm^{-1} interval, with bands located between 1000 to 1250 cm^{-1} that are assigned to the SiO$_4$ group vibrations, and shows a strong asymmetric stretching at 1071 cm^{-1}, attributed to the Si–O–Si (ν_{as}Si–O–Si) and to the terminal Si–O– (νSi–O–) bonds. The symmetric stretching Si–O–Si (ν_sSi–O–Si) vibrations appear in the 700 to 950 cm^{-1} range, while the corresponding deformation bands assigned for Si–O–Si and O–Si–O (νSiO) bonds are observed in the 400 to 700 cm^{-1} interval. A large broad band attributed to the O–H stretching vibrations, corresponding to the hydrated water molecules when interacting with the acidic centres on the inorganic surface layer, due to the presence of silanol groups, are located in the 3640 to 3590 cm^{-1} interval, followed by the water bending vibration bands in the 1670 to 1625 cm^{-1} range.[23,24] With the exchange process the sodium ions are replaced by protons and the same set of bands seen for the inorganic framework are maintained, but with a more pronounced intensity of bands in the range starting from 3200 to 3750 cm^{-1} due to silanol groups,[23,24] as illustrated in Fig. 4(b).

The organofunctionalized derivatives present very similar spectra, as shown in Fig. 4(c) and (d). The decrease in intensity of the band at 3650 cm^{-1}, derived from OH stretching vibration of the free silanol groups is clearly seen, due to the pendant silane reagents now covalently attached to the H-RUB-18 structure. Also the appearance of new bands in the 2700 to 3000 cm^{-1} range that correspond to ν(C–H) stretching vibrations in the immobilized materials are an indication of the attachment of the silylating agent to the layered surface.[25]
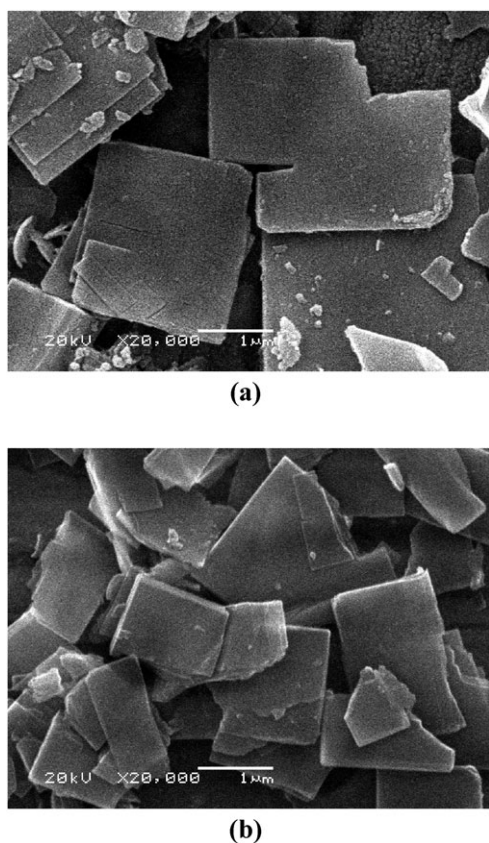
Fig. 3 Scanning electron microscopy of acidic RUB-18 (a) and of the anchored RUB-3N (b) forms.
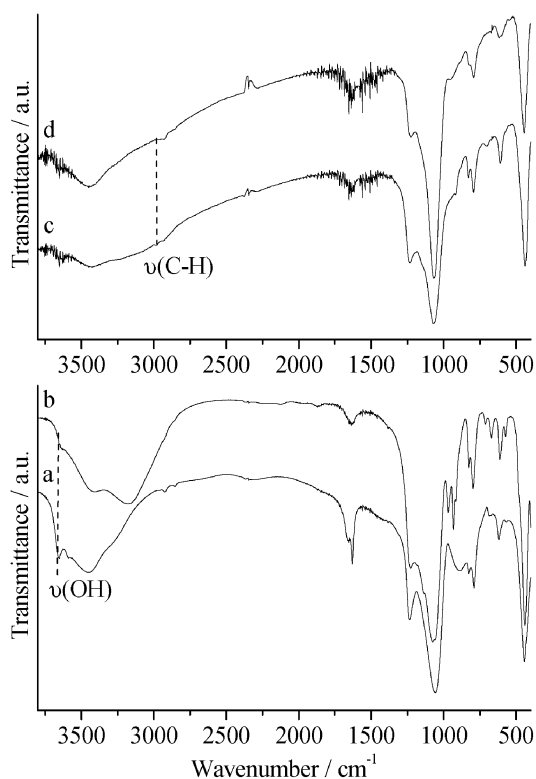

Fig. 4 Infrared spectra of Na-RUB-18 (a), H-RUB-18 (b) and the modified structures RUB-N (c), RUB-3N (d).

NMR spectroscopy has been used as a complementary technique to clarify the silicate crystal structures of this class of hydrous sodium layered silicates. For Na-RUB-18, ^{1}H, ^{23}Na and ^{29}Si NMR experiments are able to determine the nature of the hydrated water and also of hydrogen-bonding formation.[26] As a result, it is possible that the conclusions obtained for this highly ordered material would provide some information for the lowest ordered materials, such as magadiite and kenyaite. NMR is a useful technique, not only for silicates, but also to understand the structures of organo-functionalized materials.

The ^{29}Si MAS-NMR spectrum of Na-RUB-18 is shown in Fig. 5(a), where Q^4, $Si[(OSi)_4]$, and Q^3, $Si[(OSi)_3(OH)]$, units, related to the interaction of the inorganic sheets, are associated with those signals presented at -99.5 and -110.5 ppm, respectively. After the exchange reaction of the hydrated sodium by the proton, the presence of silanol groups on the surface changes the silicon environment and has displaced the Q^4 and Q^3 signals to -98.0 and -110.2 ppm,[1,26] as shown in Fig. 5(b).

For the anchored compounds, as observed through IR spectroscopy, the main inorganic structures were maintained. This fact is demonstrated by ^{29}Si MAS-NMR with signals for Q^4 and Q^3 sites, present also for the RUB-N and RUB-3N derivatives. The chemical shift of these signals are also little changed upon functionalization, being observed at -111.4 and -110.8 ppm for Q^4 and -102.9 and -99.8 ppm for Q^3 signals, as can be observed in Fig. 5(c) and (d), with also a broad signal at -98.2 and -95.5 ppm, for RUB-N and RUB-3N, respectively. The organic pendant groups covalently attached to the inorganic backbone structure gave additional signals in the silicon spectra, denoted as T^3 and T^2, related to the formation of Si–C bonds,[27] with T^3 corresponding to $[Si(OSi)_3]$ units that appeared in the -65.0 to -69 ppm interval, while T^2 corresponds to the $[Si(OSi)_2OH]$ unit, between -56.0 to -65.0 ppm. For these immobilized silicates the signals observed are very close for T^3 at -67.3 and -66.1 ppm; and for T^2 at -59.7 and -61.5, for the N and 3N derivatives, respectively.

Further evidence of the alkylsilyl groups being grafted[27] on the surface of the H-RUB-18 structure is obtained through ^{13}C NMR experiments, as shown in Fig. 6. For the chemically
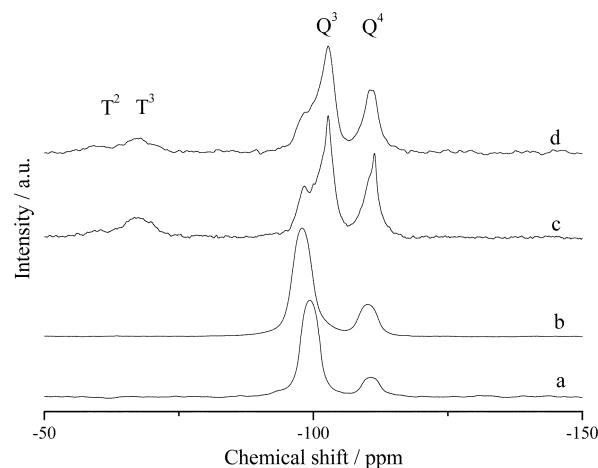

Fig. 5 ^{29}Si MAS-NMR of sodic (a) and acidic (b) RUB-18, and for the immobilized derivatives of RUB-N (c) and RUB-3N (d).
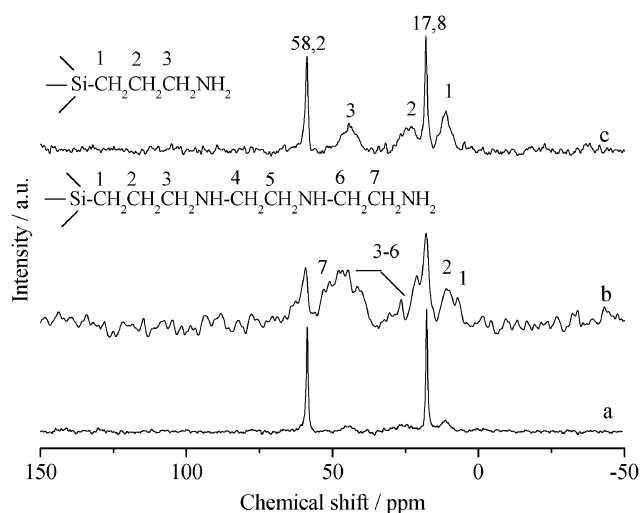
Fig. 6 ^{13}C MAS-NMR of the immobilized N (a) and 3N (b) derivatives, and HPDEC-NMR of RUB-N (c).

modified materials RUB-N and RUB-3N, the spectra showed two distinct signals at 58.2 and 17.8 ppm, related to the carbons from the ethanol used in the washing which it was not possible to eliminate even after drying under vacuum at 348 K for 8 h, which indicates that the ethanol is probably retained inside the pore structure. This set of results corroborates with the X-ray patterns, suggesting that the functionalization occurred mainly on the external surface. It seems these signals are not related to unhydrolyzed groups in the functionalization process that are shown for RUB-3N. This hypothesis is corroborated by the existence of only one signal from the methoxy group of this specific molecule. In addition, as is well known, the used silylating agents are readily covalently bonded on surfaces due to the easy hydrolysis of alkoxide groups.

The three-carbon spacer groups for the RUB-N material gave distinct signals, C1, C2 and C3 at 11.1, 23.5 and 44.8 ppm, as could be seen through the HPDEC ^{13}C spectrum for this sample, as shown in Fig. 6(c). The long chain pendant attached molecule in RUB-3N led to a more complex spectrum, with the carbon atoms C1 and C2, belonging to the spacer group appearing at 6.5 and 10.7 ppm, respectively. The sequence of carbon atoms 3–6 gave an intense peak at 45.5 ppm, followed by shoulders at 41.3 and 25.9 ppm, while the seventh carbon atom gave a peak at 53.5 ppm, as shown in Fig. 6(b). This sample shows also only a small amount of ethanol, probably because the final material was particularly exfoliated according to the X-ray data, the pore structure was disorganized and the structure retains less ethanol.

The available basic nitrogen atoms attached to the pendant molecules covalently bonded to the inorganic framework are useful for cation removal from aqueous solutions, especially when chelating effects are present.[28] As a result, the divalent cations copper, nickel and cobalt were analysed in the sorption process. The properties for extracting cations from aqueous solution were evaluated by measuring sorption isotherms, whose capacity (N_f) was calculated by means of eqn (1):

$$N_f = (n_I - n_s)/m \qquad (1)$$

where n_i and n_s are the initial and final number of moles of metal (mol dm^{-3}) in solution, respectively, and m is the mass (g).

To evaluate the results obtained from the isotherms of sorption, the data were adjusted to the Freundlich model,[28] describing a heterogeneous system, whose linearized form is expressed by eqn (2):

$$\log N_f = \log K_F + (1/n)\log C_S \qquad (2)$$

where N_f was defined as above, C_S (mmol dm^{-3}) is the concentration of cation in the supernatant in equilibrium, directly related to n_s, K_F (dm^3 g^{-1}) is the Freundlich constant, and $1/n$ is the heterogeneity factor. K_F and n affinity constants are empirical in nature and depend on environmental factors.

The isotherms of sorption were represented by N_f as a function of C_S as shown in Fig. 7 for copper adsorption in the modified RUB-N layered material. The n constant obtained through the Freundlich approach enables application of the Langmuir–Freundlich model,[29] given by eqn (3):

$$\frac{(C_S)^{1/n}}{N_f} = \frac{1}{N_S b} + \frac{(C_S)^{1/n}}{N_S} \qquad (3)$$

where C_S, N_f and n were defined as above, N_S (mmol g^{-1}) is the maximum adsorption capacity of metals per gram of material, which depends on the number of sorption sites, and b is a constant related to chemical equilibrium at the solid/liquid interface. The N_S and b values for each sorption isotherm were obtained from the angular and linear coefficients, respectively, of the linearized form of the isotherms, by plotting $(C_S)^{1/n}/N_f$ $vs.$ $(C_S)^{1/n}$. The linearized Langmuir–Freundlich isotherm is shown in Fig. 8. The quantitative data were obtained through applying the Freundlich and Langmuir–Freundlich models and are listed in Table 2.

The sorption capability of some natural and synthesized sorbents and the inorganic–organic hybrids obtained from H-RUB-18 for divalent cation removal are given in Table 3. With the exception of diethylenetriamine functionalized H-kenyaite for copper, nickel and cobalt, the present results are higher in comparison to other organofunctionalized
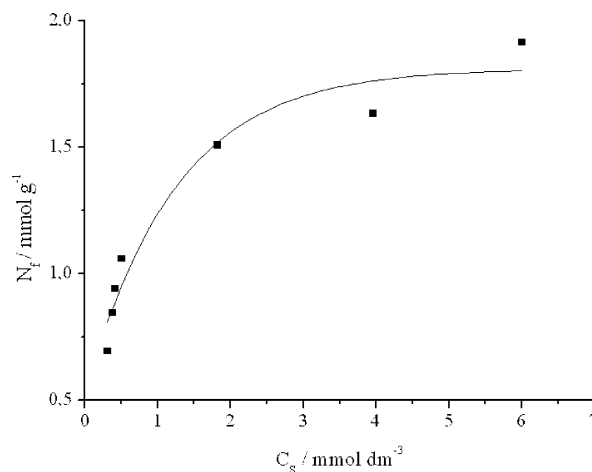

Fig. 7 Sorption isotherm of Cu^{2+} on the RUB-N organo-modified surface.
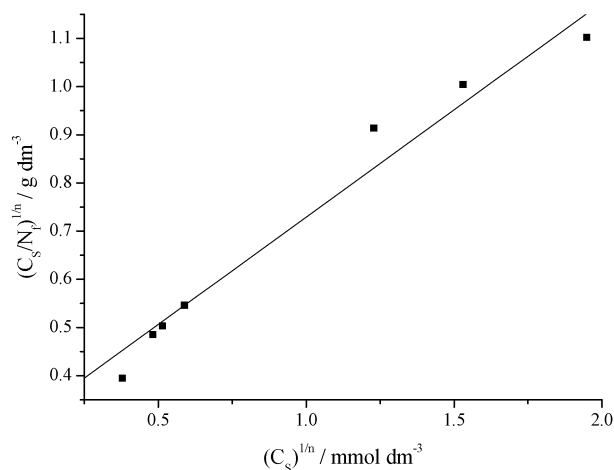
Fig. 8 Linearized Langmuir–Freundlich sorption isotherm of Cu^{2+} on RUB-N.

Fig. 9 Calorimetric titration of 0.0196 g of RUB-3N suspended in 2.0 cm^3 of water with 0.104 mol dm^{-3} Cu^{2+} in the same solvent at 298.15 $\pm$ 0.20 K. The curves of the calorimetric titration are represented by the sum of the thermal effects of the metal titration $\sum Q_t$ (■), dilution $\sum Q_d$ (●) and the resulting thermal effects $\sum Q_r$ (▲). $\sum Q$ and V_{ad} values are the sum of the detected thermal effect and total injected volume of metal solution, respectively.

Table 2 Sorption of divalent cations (M^{2+}) on chemically modified H-RUB-18 fitted by the Freundlich and Langmuir–Freundlich models to obtain equilibrium sorption capacities (N_f/mmol g^{-1}), sorption capacities of saturation (N_S/mmol g^{-1}), the constants b, n, K_F and the correlation coefficient (R^2)

Material	M^{2+}	Freundlich			Langmuir–Freundlich			
		K_F	n	R^2	N_f	N_S	B	R^2
RUB-N	Cu	2.104	2.28	0.9841	2.01	2.24	1.57	0.9669
	Ni	2.016	2.14	0.9576	2.30	2.34	1.22	0.9886
	Co	1.149	3.16	0.9719	1.57	1.57	2.06	0.9966
RUB-3N	Cu	0.909	2.86	0.9882	1.62	1.69	1.22	0.9951
	Ni	0.871	4.83	0.9524	1.28	1.28	3.10	0.9953
	Co	0.744	4.59	0.9349	1.23	1.28	2.67	0.9911

sorbents, showing a favorable capacity of these layered materials for metal cation removal from aqueous solutions at the solid/liquid interface.

The resulting thermal effects (Q_r) obtained from metal nitrate interaction with organofunctionalized RUB-18 derivatives were determined through calorimetric experiments,[33] by subtracting the cation dilution effect (Q_d) and the effect of the inorganic support (Q_s) in water from the total thermal effect (Q_t), as given by eqn (4):

$$\sum Q_r = \sum Q_t - \sum Q_d - \sum Q_s \qquad (4)$$

For the net thermal effect the contribution of the inorganic support gave a null value, as normally observed.[11–13] The isotherms obtained for copper are shown in Fig. 9 for the layered RUB-3N material. For nickel and cobalt sorptions with the chemically modified RUB-N material, the same isotherms w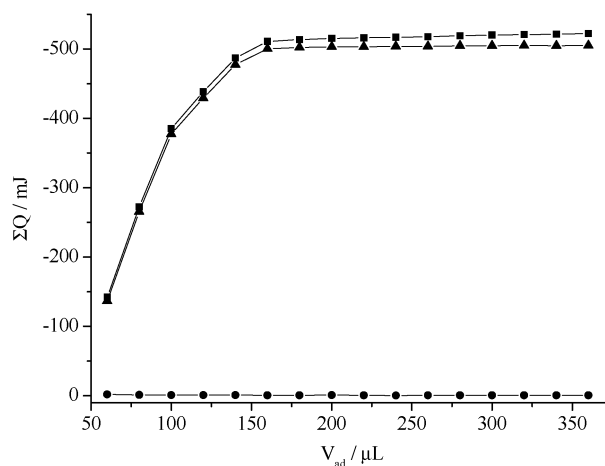ere obtained, but the thermal effect gave exothermic and endothermic signals, resulting in a near null total sum and, consequently, resulted in a large error in the calculations, so that it was not possible to determine the thermochemical data of these interactions.

The change in enthalpy for cation/material interaction can be obtained by applying the calorimetric sorption data of the modified Langmuir[34] equation:

$$\frac{\sum X}{\sum \Delta_R h} = \frac{1}{(K-1)\Delta_{int}h} + \frac{X}{\Delta_{int}h} \qquad (5)$$

where $\sum X$ is the sum of the mole fraction of the cation in solution after sorption, with X obtained for each point of titrant addition; $\Delta_R h$ (J mol^{-1}) is the integral thermal effect resulting from the net titration process and K is a proportionality constant that also includes the equilibrium constant.

Through the angular and linear coefficients from the $\sum X/\sum \Delta_R h$ as a function of $\sum X$ plot, it is possible to obtain $\Delta_{int}H$ and K values, respectively. Thus, the molar enthalpy of the sorption process[34] is calculated by eqn (6), with N_S obtained from eqn (3):

$$\Delta H = \Delta_{int}h/N_S \qquad (6)$$

From K values, the Gibbs free energy[34] were calculated from eqn (7):

$$\Delta G = -RT \ln K \qquad (7)$$

Table 3 Comparison of the maximum sorption capability (N_S) for divalent cations (M^{2+}) for some sorbents

Sorbent	N_S (Cu^{2+})/mmol g^{-1}	N_S (Ni^{2+})/mmol g^{-1}	N_S (Co^{2+})/mmol g^{-1}	Ref.
Ponkan peel	1.310	1.920	1.370	30
Chitosan	0.380	0.370	0.270	31
Aminopropyl functionalized H-kenyaite	0.760	0.620	0.570	32
Diethylenetriamine functionalized H-kenyaite	1.190	1.140	1.040	32
Aminopropyl functionalized H-RUB-18	2.104	2.016	1.149	This work
Diethylenetriamine functionalized H-RUB-18	0.909	0.871	0.744	This work

From these values the entropy[34] can be then calculated:

$$\Delta G = \Delta H - T\Delta S \qquad (8)$$

All thermodynamic results are listed in Table 4. The enthalpic data are exothermic for all sorption processes of organo-functionalized RUB-18 and this behaviour is expected and associated with the availability of the free amino groups attached to the pendant chain covalently bonded on the inorganic surface to interact with cations in solution at the solid/liquid interface. The negative free Gibbs energy indicates a spontaneity of the process with positive entropic values.[31,32] The high entropic values for all sorption processes listed in Table 4 are associated with the displacement of water molecules initially bonded not only to the cations, but also to the basic nitrogen atoms attached to the pendant chains, during the cation/basic center interactions, to cause a disorganization of the system, as observed before.[35–38] Thus, the net thermodynamic data consisted in considering individual contributions of enthalpy and entropy to determine the final behaviour. In the present case, the less favourable enthalpic value for RUB-N relative to RUB-3N is compensated by the high positive entropic value. For nickel and cobalt sorption by the RUB-3N material, these interactions continue to be entropically favourable, as also observed for copper in the same chemically modified silicic acid, however, with a relevant enthalpic contribution.

Experimental

Chemicals

The reactants, such as silica gel (Aldrich) and sodium hydroxide (Vetec) used for Na-RUB-18 synthesis were reagent grade. Hydrochloric acid (Nuclear) was used for the proton exchange process. The solvent xylene (Synth) was used without further purification. The silylating agents (Aldrich) 3-aminopropyltriethoxysilane (N), $(CH_2CH_3O)_3Si(CH_2)_3NH_2$ and N-3-trimethoxysilylpropyldiethylenetriamine (3N), $(CH_3O)_3Si(CH_2)_3NH(CH_2)_2NH(CH_2)_2NH_2$ were used as received for the silylation procedure.

Synthesis of Na-RUB-18

The layered sodic silicate Na-RUB-18 was obtained from a suspension of silica gel and sodium hydroxide solution with a molar ratio of $SiO_2 : NaOH : H_2O$ of $1 : 0.5 : 7$, as typically indicated, 25.0 g of SiO_2 for 8.32 g of NaOH dissolved in 53 cm^3 of water. The gel was transferred to a stainless steel autoclave lined with Teflon for hydrothermal treatment during 9 days at 378 K. Then, the solid was filtered off and washed with doubly distilled water until neutral pH and air dried.[8,39]

Synthesis of H-RUB-18

Na-RUB-18 (3.0 g) was dispersed in 300 cm^3 of 0.20 mol dm^{-3} of aqueous hydrochloric acid and the mixture was aged at room temperature for 6 h. Then the white product was separated by centrifugation (3000 rpm for 5 min) and finally washed with doubly distilled water until neutral pH.[39]

Organofunctionalization

H-RUB-18 (1.0 g) was dried for 6 h on a vacuum line to remove any water condensed on the surface, making the silanol groups available for reaction, and then was dispersed in 1.0 cm^3 of silylating agent dissolved in 50 cm^3 of xylene. The mixture was stirred in the 333–343 K interval of temperature under a nitrogen flow during five days, a procedure that is similar to that used in the phyllosilicate organofunctionalization process.[29] The control of temperature at about 343 K must be maintained, since it is already known that the process of material hydration and re-hydration is maintained under such conditions.[23] The product was separated by centrifugation, washed with ethanol and with doubly distilled water, and finally dried under vacuum at 343 K for 8 h. The procedure for the anchoring was repeated one more time to achieve higher amounts of silylating agent incorporation and the products of the reactions are denoted RUB-N and RUB-3N, for (N) and (3N) silylating agents, respectively.

Sorption of metal ions

Aqueous solutions of the divalent metallic cations copper, nickel and cobalt were used to obtain the isotherms of sorption through the batchwise process, by stirring 20 mg of the chemically immobilized RUB-18 (N or 3N) materials in 25.0 cm^3 of cation solution, varying from 0.70 to 7.0 mmol dm^{-3} for 24 h at 298 ± 1. The cation solutions were prepared by dissolving the respective nitrate salts in deionized water, to give a final pH of 4.5. After the adsorption process, aliquots were removed from the supernatant for cation determination through ICP-OES.

Calorimetric titration

The thermal effects of interactions involving the divalent cations copper, nickel and cobalt with the organofunctionalized basic centers were measured through a titration method,[29] using a Thermometric 2277 calorimetric system. For each measurement, a sample of about 20 mg of chemically modified H-RUB-18 was suspended in 2.0 cm^3 of distilled water under stirring and thermostated at 298.15 ± 0.20 K. The titration was done by successive addition of 20.0×10^{-3} cm^3 increments of the titrant consisting of 0.10 mol dm^{-3} of each metal nitrate solution. The thermal effect, Q_t (J), was determined after each increment of titrant. Under the same experimental conditions

Table 4 Thermochemical data of cation (M^{2+}) interaction with chemically modified silicic acid materials

Material	M^{2+}	$-\Delta_{int}h$/J g^{-1}	$-\Delta H$/kJ mol^{-1}	K	$-\Delta G$/kJ mol^{-1}	ΔS/J K^{-1} mol^{-1}
RUB-N	Cu	1.84	0.82 ± 0.50	2.10×10^6	35.9 ± 0.2	121 ± 1
RUB-3N	Cu	27.00	15.98 ± 0.20	2.03×10^6	36.0 ± 0.7	67 ± 1
	Ni	13.67	10.68 ± 0.20	7.46×10^6	39.2 ± 0.3	96 ± 1
	Co	26.80	20.94 ± 0.50	1.01×10^7	40.0 ± 0.4	64 ± 1

the corresponding thermal effect of the dilution of the cation solution in the absence of modified material, Q_d (J) was also obtained.

Characterization

The percentages of carbon, hydrogen and nitrogen were determined with a Perkin-Elmer 2400 Series II microelemental analyzer and at least two independent determinations were performed for each sample.

X-Ray powder diffraction measurements were obtained on a Shimadzu XRD-6000, with Cu-Kα (λ = 0.154 nm) radiation (40 kV, 30 mA), at a scan rate of $3.33 \times 10^{-2} \, ^\circ \, s^{-1}$ at room temperature, with 2θ varying from 1.4 to 50°.

Thermogravimetric measurements were made on a TA Instruments 5100, with a heating rate of 0.167 K s^{-1}, starting at room temperature until 1273 K, under 1.67 cm^3 s^{-1} of argon flow.

Scanning electron microscopy measurements were obtained with a Jeol 6360-LV apparatus, operating at 20 kV. The samples were deposited from a suspension in acetone solution onto a gold support and sputter deposited prior the SEM analyses.

Infrared spectra were measured on a MB-Series model Bomem FTIR spectrometer, using pressed KBr pellets with a pressure of 5 tonnes cm^{-2}, with 32 scans in the 4000–400 cm^{-1} range, and resolution of 4 cm^{-1}.

Solid-state NMR spectra were obtained for ^{29}Si and ^{13}C nuclei on a Bruker AC 300/P solid-state high-resolution spectrometer, by cross-polarization and magic angle spinning (CP-MAS), at a frequency of 59.6 MHz and with a rotational frequency of 15 kHz, acquisition time of 66 ms and contact time of 5 ms for the ^{29}Si nucleus. A frequency of 75.5 MHz was used with an acquisition time of 78 ms and contact time of 3 ms for the ^{13}C nucleus. High-power decoupling (HPDEC) was applied for ^{13}C MAS NMR for the RUB-N sample. Chemical shifts were referenced to tetramethylsilane (TMS).

A Perkin-Elmer model OPTIMA 3000 DV inductively coupled plasma optical emission spectrometer was used to determine the amount of divalent copper, nickel and cobalt cations in the supernatant after the sorption process.

Conclusions

New lamellar inorganic–organic hybrids were successfully synthesized from acidic RUB-18 and reveal well-organized crystalline materials with an increasing H-RUB-18 basal distance, due to the accommodation of silane reagents inside the layers for RUB-3N or mostly on the surface for RUB-N. Elemental analysis, thermogravimetry and IR spectroscopy confirm the presence of covalent bond formation, providing convincing proof of the silylation process, with insights in morphology through SEM micrographs.

Structural data associated with NMR, mainly of the silicon nucleus in the solid state, showed the inorganic layer arrangement and silicon–carbon covalent bond formation, assigned to the success of the chemical modification process, as indicated by the presence of T^2 and T^3 units on the surface.

The methodology of the organofunctionalization reaction was the same as for phyllosilicate modifications, but with the advantage of using mild conditions of temperature and small amounts of silylating agents. This procedure infers the possible use of this route to attach other kinds of silylating pendant groups onto other inorganic lamellar systems.

The efficiency of the modified materials for cation sorption was evaluated through a batchwise process, demonstrating the ability of cation removal from waste water and industrial effluents, while the thermodynamic values suggest a favourable process due to the exothermic enthalpy, negative free Gibbs energy and positive entropy values.

The results obtained pointed out that depending on the silylating agent used different inorganic–organic hybrids can be successfully synthesized with great possibilities to explore the functionality incorporated in the new materials for practical applications.

Acknowledgements

References

1 M. Borowski, O. Kovalev and H. Gies, *Microporous Mesoporous Mater.*, 2008, **107**, 71–80.
2 G. Lagaly and K. Beneke, *Colloid Polym. Sci.*, 1991, **269**, 1198–1211.
3 J. M. Rojo and E. Ruiz-Hitzky, *Nature*, 1980, **287**, 28–30.
4 L. Mercier and T. J. Pinnavaia, *Microporous Mesoporous Mater.*, 1998, **20**, 101–106.
5 G. Borbély, H. K. Beyer, H. G. Karge, W. Schwieger, A. Brandt and K.-H. Bergk, *Clays Clay Miner.*, 1991, **39**, 490–497.
6 H. Annehed, L. Falth and F. J. Lincoln, *Z. Kristallogr.*, 1982, **159**, 203–210.
7 L. A. J. Garvie, B. Devouard, T. L. Groy, F. Camara and P. R. Buseck, *Am. Mineral.*, 1999, **84**, 1170–1175.
8 W. Schwieger, D. Heidemann and K.-H. Bergk, *Rev. Chim. Miner.*, 1985, **22**, 639–649.
9 S. Vortmann, J. Rius, S. Siegmann and H. Gies, *J. Phys. Chem. B*, 1997, **101**, 1292–1297.
10 M. Richard-Plouet, S. Vilminot and M. Guillot, *New J. Chem.*, 2004, **28**, 1073–1082.
11 M. G. Fonseca and C. Airoldi, *J. Colloid Interface Sci.*, 2001, **240**, 229–236.
12 M. G. Fonseca and C. Airoldi, *Mater. Res. Bull.*, 2001, **36**, 277–287.
13 J. A. A. Sales, A. G. S. Prado and C. Airoldi, *Surf. Sci.*, 2005, **590**, 51–62.
14 C. Sanchez, B. Julian, P. Belleville and M. Popall, *J. Mater. Chem.*, 2005, **15**, 3559–3592.
15 K. W. Park, S. Y. Jeong and O. Y. Kwon, *Appl. Clay Sci.*, 2004, **27**, 21–27.
16 Y. Ide and M. Ogawa, *Chem. Commun.*, 2003, 1262–1263.
17 A. Shimojima, D. Mochizuki and K. Kuroda, *Chem. Mater.*, 2001, **13**, 3603–3609.
18 S. Okutomo, K. Kuroda and M. Ogawa, *Appl. Clay Sci.*, 1999, **15**, 253–264.
19 Z. Wang and T. J. Pinnavaia, *J. Mater. Chem.*, 2003, **13**, 2127–2131.
20 Y. Ide, A. Fukuoka and M. Ogawa, *Chem. Mater.*, 2007, **19**, 964–966.
21 D. Mochizuki, A. Shimojima and K. Kuroda, *J. Am. Chem. Soc.*, 2002, **124**, 12082–12083.
22 E. F. Vansant, P. Van Der Voort and K. C. Vranken, *Characterization and Chemical Modification of the Silica Surface*, Elsevier, Amsterdam, 1995.
23 M. F. Iozzi, C. Bisio, T. R. Macedo, C. Airoldi, M. Cossi and L. Marchese, *J. Mater. Chem.*, 2009, **19**, 2610–2617.

24 Y. Huang, Z. Jiang and W. Schwieger, *Chem. Mater.*, 1999, **11**, 1210–1217.

25 C.-M. Leu, Z.-W. Wu and K.-H. Wei, *Chem. Mater.*, 2002, **14**, 3016–3021.

26 I. Wolf, H. Gies and C. A. Fyfe, *J. Phys. Chem. B.*, 1999, **103**, 5933–5938.

27 A. S. O. Moscofian and C. Airoldi, *J. Hazard. Mater.*, 2008, **160**, 63–69.

28 B. Royer, N. F. Cardoso, E. C. Lima, V. S. O. Ruiz, T. R. Macedo and C. Airoldi, *J. Colloid Interface Sci.*, 2009, **336**, 398–405.

29 S. Azizian, M. Haerifar and J. Basiri-Parsa, *Chemosphere*, 2007, **68**, 2040–2046.

30 F. A. Pavan, I. S. Lima, E. C. Lima, C. Airoldi and Y. Gushikem, *J. Hazard. Mater.*, 2006, **137**, 527–533.

31 I. S. Lima and C. Airoldi, *Thermochim. Acta*, 2004, **421**, 133–139.

32 V. S. O. Ruiz, G. C. Petrucelli and C. Airoldi, *J. Mater. Chem.*, 2006, **16**, 2338–2346.

33 C. R. Silva, M. G. Fonseca, J. S. Barone and C. Airoldi, *Chem. Mater.*, 2002, **14**, 175–179.

34 M. A. Melo Junior, F. J. V. E. Oliveira and C. Airoldi, *New J. Chem.*, 2009, **33**, 1038–1046.

35 T. R. Macedo and C. Airoldi, *Microporous Mesoporous Mater.*, 2006, **94**, 81–88.

36 D. L. Guerra, R. R. Viana and C. Airoldi, *Mater. Res. Bull.*, 2009, **44**, 485–491.

37 A. M. Lazarin and C. Airoldi, *J. Chem. Thermodyn.*, 2009, **41**, 21–25.

38 E. C. N. Lopes, K. S. Sousa and C. Airoldi, *Thermochim. Acta*, 2009, **483**, 21–28.

39 K. Kosuge and A. Tsunashima, *J. Chem. Soc., Chem. Commun.*, 1995, 2427–2428.